Alfvén Wave Transport Effects in the Time Evolution of Parallel Cosmic-Ray Modified Shocks

T. W. Jones

Department of Astronomy, University of Minnesota, Minneapolis, MN 55455

To be published in the Astrophysical Journal August 20, 1993

ABSTRACT

This paper presents a numerical study of the time evolution of plane, cosmic-ray modified shocks with magnetic field parallel to the shock normal, based on the diffusive shock acceleration formalism and including the effects from the finite propagation speed and energy of Alfvén waves responsible for controlling the transport of the cosmic-rays. The simulations discussed are based on a three-fluid model for the dynamics, but a more complete formalism is laid out for future work. The results of the simulations confirm earlier, steady state analyses that found these Alfvén transport effects to be potentially important when the upstream Alfvén speed and the gas sound speed are comparable; *i.e* when the plasma and magnetic pressures are similar. It is also clear, however, that the impact of Alfvén transport effects, which tend to slow shock evolution and reduce the time asymptotic cosmic-ray pressure in the shock, is strongly dependent upon uncertain details in the transport models. Both cosmic-ray advection tied to streaming Alfvén waves and dissipation of wave energy are important to include in the models. Further, Alfvén transport properties on both sides of the shock are also influential.

subject headings: acceleration of particles - cosmic-rays - hydrodynamics - shock waves - Alfvén waves

1. INTRODUCTION

Diffusive acceleration associated with shocks is now the most widely discussed mechanism for acceleration to high energies of charged particles (hereafter, cosmic-rays or CR) in a wide range of astrophysical settings. At least in idealized treatments the mechanism apparently can be both efficient at capturing gas kinetic energy and robust in certain important characteristics, such as the momentum distribution of the accelerated charged particles (see, for example, the reviews by Blandford & Eichler 1987, Jones & Ellison 1991). Looked at closely, however, the physics is complex and generally nonlinear. Furthermore, although much of our basic understanding of diffusive acceleration has been derived from steady state analyses (*e.g.* Drury and Völk 1981; Völk, Drury & McKenzie 1984 [hereafter VDM]), it has become increasingly clear that time dependent studies are necessary in many circumstances (e.g., Jones and Kang 1992a). This comes about for a variety of reasons including the likelihood that many shocks do not have time to reach a steady state or simply cannot develop truly steady properties (*e.g.*, Jones and Kang 1992b, 1993).

The diffusive acceleration process depends upon the existence of rapid pitch angle redistribution by way of scattering both upstream and downstream of the shock. This scattering is generally assumed to be primarily resonant scattering with Alfvén waves, since those waves can be directly generated by the CR, and, being noncompressive, are weakly damped in the background plasma, so long as the plasma is fully ionized and the gas sound speed, c_s, is not exceeded by the Alfvén speed, v_A, (Chin & Wentzel 1972, Skilling 1975b, Ferrière *et al.* 1988). In the strong scattering limit the CR will become nearly isotropized with respect to the rest frame of the Alfvén waves. When the CR are not quite isotropic, so that if they are streaming in that frame, the CR will amplify these same Alfvén waves by the resonant scattering process. For shocks wave growth is probably strongest in the shock precursor and, sometimes, immediately behind the shock jump, where gradients in the CR distribution maintain some streaming. The waves generated in this fashion in turn will transfer momentum, energy and, through dissipation, entropy to the plasma. The basics of those interactions are well known, at least through quasi-linear theory (*e.g.* . Skilling 1975a,b,c, Bell 1978, Achterberg 1982, McKenzie and Völk 1982, Schlickeiser 1992). The possibility that the waves may themselves be dynamically important also has been recognized for some time (*e.g.*, McKenzie and Völk 1982, Achterberg 1982, VDM).

There are a number of ways that Alfvén waves can directly influence the evolution of a CR mediated shock. First is the already mentioned likelihood that at least some of the energy taken from the CR to generate Alfvén waves will be locally dissipated within the gas. Not only does that directly remove energy from the CR and transfer it back to the gas, but in addition it alters the shock by changing the properties of the gas in the shock transition. In particular, the gas is hotter entering the shock, so the effective Mach number of the shock is diminished, thereby reducing the expected efficiency of the CR acceleration process (Drury & Völk 1981; Achterberg, Blandford & Periwal 1984). Advection of the scattering centers with respect to the gas is also very important, since it alters the characteristic time that particles spend on either side of the shock and the

particle speed change associated with a shock crossing if the drift speed changes across the shock transition. That changes the mean rate at which particles are accelerated. If the wave energy and pressures are large enough they can have direct dynamical impact on the gas flow and the associated CR acceleration. All these effects can be conveniently collected together under a heading, "Alfvén cosmic-ray transport". VDM used a two-fluid model to estimate the steady state acceleration efficiency of shocks including Alfvén transport terms. Their calculations showed that Alfvén transport effects tend to produce a significantly hotter downstream gas state and a reduced CR acceleration efficiency if the upstream Alfvén speed is comparable to the upstream gas sound speed. Such an upstream condition is quite plausible in the interstellar medium, for example (*e.g.*, Spitzer 1978). This could be important, both in terms of the amount of energy that might be expected to be transferred to CR and to the predicted state of the postshock gas. Calculations of steady, CR modified shocks not including Alfvén transport have found such high acceleration efficiencies that the CR pressure can completely smooth out the transition for moderate to strong shocks; thus, leading to rather cool gas downstream (*e.g.*, Drury and Völk 1981, Jones & Kang 1990 [hereafter JK90]). The VDM models with Alfvén transport reduced the efficiency enough when $c_s \sim v_A$ that the gas subshock was restored, except at very large Mach numbers. However, despite this suggestion that Alfvén transport may be an important effect in some circumstances, the presence of the Alfvén waves beyond their scattering role has been more often ignored even in steady state treatments of diffusive acceleration. To date only the role of entropy production in the gas through wave dissipation has been modeled in any nonlinear, time dependent treatments (Markiewicz *et al* 1990, Dorfi 1991). This neglect has been due partly to the fact that nonlinear diffusive shock acceleration theory is already an intricate problem and because some important details of Alfvén transport, such as the damping of the waves are not very well understood. But, it is important to understand more fully how significant the consequences of Alfvén transport may be and how generally and accurately it must be included for accurate assessment of CR acceleration in both steady and unsteady shocks.

My goal in the present paper is to explore qualitatively some of the issues associated with a more complete treatment of Alfvén transport in CR shocks. The treatment is still simplified in some important respects, but I have examined some new issues and have included for the first time in a nonlinear, time dependent study of plane CR mediated shocks both the entropy producing effects of wave dissipation and effects due to the Alfvén wave advection of the CR relative to the gas. I also begin examination of the direct consequences of including the pressure and energy of the Alfvén waves in the formalism.

In §2 I outline some important features of the theory and discuss a "three-fluid" model that I have applied as a first step to time dependent studies. The characteristics of some example model calculations are specified in §3; results from those calculations are described in §4, while §5 provides a brief summary of conclusions.

2. BASIC RELATIONS

The fluid approach to modeling CR transport depends upon the standard compressible flow conservation laws for the underlying plasma (gas) augmented by terms representing the back reaction of the CR and the Alfvén wave field and by transport equations for the CR and the waves. In the present study I will investigate only plane shock structures of at least moderate strength whose normals are parallel to the mean magnetic field and which are propagating into a warm or hot plasma, so that sonic mode (hydrodynamic) shocks are present. This is a significant restriction, of course, but a necessary beginning in sorting through some very complex phenomena. However, I want to focus on the interaction of Alfvén waves with the plasma and the CR. Thus, the Euler's equation for the plasma must include the pondermotive force from the Alfvén waves. As shown by Achterberg (1982), for example, this gives

$$\frac{d\vec{u}}{dt} = -\frac{1}{\rho}\vec{\nabla}(P_g + P_c + \frac{1}{2}E_w), \qquad (2.1),$$

where $\vec{u}$ is the velocity of the plasma, $E_w = 2P_w = (\delta B)^2/(4\pi)$ is the energy density per unit volume in Alfvén waves and δB represents the wave-number integrated magnetic field fluctuation, while P_g, P_c and P_w are the pressures of the gas, the CR and the waves, respectively. The Lagrangian time derivative incorporating plasma motion is $d/dt = \partial/\partial t + \vec{u}\cdot\vec{\nabla}$. The back reaction of CR on the gas, represented through $-\vec{\nabla}P_c$, is explicitly and automatically included through the pondermotive force, since resonant scattering of CR off the Alfvén waves directly transfers momentum to the gas. The equation for energy conservation in the gas under these circumstances is

$$\frac{de}{dt} = -\frac{1}{\rho}\vec{\nabla}\cdot\{(P_g + P_c + P_w)\vec{u}\} + \frac{1}{\rho}(P_c + P_w)\vec{\nabla}\cdot\vec{u} + \frac{L-S}{\rho}. \qquad (2.2)$$

Here, e is the sum of gas thermal and kinetic energy per unit mass. The terms L and S represent nonadiabatic heating from dissipation of the Alfvén waves and energy lost to CR through the injection of gas particles at low energy into the CR spectrum. I will assume a standard equation of state for the gas, $P_g = (\gamma_g - 1)E_g$, with $\gamma_g = 5/3$ and ignore radiative cooling or thermal conduction. The usual mass conservation equation for the gas also applies:

$$\frac{d\rho}{dt} = -\rho\vec{\nabla}\cdot\vec{u}. \qquad (2.3)$$

Inertia in the CR component is neglected, since it is commonly supposed that the number of CR ions is very small compared to the number of "gas" ions. As shown, for example, by Skilling (1975a) the transport equation for an almost isotropic CR particle distribution in the limit of strong scattering is a diffusion-advection equation,

$$\frac{df}{dt} = \frac{1}{3}\left[\vec{\nabla}\cdot(\vec{u} + \vec{u}_w)p\frac{\partial f}{\partial p}\right] + \vec{\nabla}\cdot(\kappa\vec{\nabla}f) - (1 + \frac{1}{3}\frac{\partial lnu_w}{\partial lnp})\vec{u}_w\cdot\nabla f + Q, \qquad (2.4)$$

where $f(x,p,t)$ is the number density of particles in phase space. The source term Q represents particle injection from the gas and is related to the term S in equation [2.2] (see

equations [2.8] and [2.9] in Kang & Jones 1991). In addition, the mean CR streaming or "Alfvén advection" velocity relative to the gas, $\vec{u}_w(p)$, is

$$\vec{u}_w = \frac{3}{2}\left\langle (1-\mu^2)\frac{\nu_+ - \nu_-}{\nu_+ + \nu_-}\right\rangle v_A\hat{n} =$$

$$h_w\frac{\nu_{+o} - \nu_{-o}}{\nu_{+o} + \nu_{-o}}v_A\hat{n} = h_w\frac{E_{wk+o} - E_{wk-o}}{E_{wk+o} + E_{wk-o}}v_A\hat{n}, \tag{2.5}$$

where $v_A = B/\sqrt{4\pi\rho}$ is the Alfven speed, and $v = pc/\sqrt{p^2+m^2c^2}$ is the speed of the scattered particle.

The mean rates for resonant scattering, $\nu_\pm$, between CR particles of momentum along the magnetic field, $p\mu = \vec{p}\cdot\hat{n} = \Omega_o m/k$, and Alfvén waves of wave number, k, traveling in the two directions along the field $\pm\hat{n} = \pm\vec{B}/B$ are

$$\nu_\pm = \frac{\pi}{4}\frac{\Omega_o m v}{p}\frac{kE_{wk\pm}}{E_B} = \frac{\pi}{4}\frac{v}{r_L}\frac{kE_{wk\pm}}{E_B}. \tag{2.6}$$

Ω_o is the nonrelativistic cyclotron frequency, r_L is the particle Larmour radius and $E_B = B^2/(8\pi)$. Furthermore, $E_{w\pm} = \int E_{wk\pm}dk$ is the total energy density of waves propagating in the same two directions. The angular brackets in equation [2.5] represent an average over μ. The factor h_w and the subscript $_o$ in the last two expressions for $\vec{u}_w$ have been introduced to allow us to represent the pitch angle average in terms of the scattering rate $\nu_{\pm o}$ from Alfvén waves at the shortest wavelength resonant at a given momentum; namely $k \approx \Omega_o m/p$.

If the ratio of $E_{wk+}/E_{wk-} = \nu_+/\nu_-$ is independent of k or if one of $E_{wk\pm}$ is dominant at the appropriate wave numbers, $h_w = 1$ and in equation [2.4] $\partial lnu_w/\partial lnp = 0$, which leads to considerable simplifications in some of the following relations. In evaluating the diffusion coefficient, κ, and eventually the growth rate of Alfvén waves (equation [2.10]) it is convenient to adopt the approximation that the scattering is dominated by $\nu_{\pm o}$ (*e.g.*, Skilling 1975c, Lee 1983). As argued by Lee (1983) this choice is probably adequate and consistent with needed corrections to quasilinear theory under most circumstances, so long as E_{wk} does not vary dramatically in the range of wavenumbers resonant with the bulk of the CR at a given momentum. It does capture the important physical point that the scattering rate should scale inversely with the intensity of Alfvén waves. Then the CR diffusion coefficient parallel to the magnetic field, $\kappa = \kappa(p)$, is given by

$$\kappa(p) \approx \frac{v^2}{3}\frac{1}{\nu_{+o} + \nu_{-o}}, \tag{2.7}$$

In equation [2.5] the factor $h_w \approx 1$ in this approximation, as well. This approximation for $\nu_\pm$ will be used for the remainder of our discussion, and the extra subscript $_o$ on the scattering rates will be implicit. For further details about the derivation of equations [2.4 - 2.7] the reader is referred to Skilling (1975a).

The $\vec{u}_w$ terms in equation [2.4] come about because the scattering by Alfvén waves tends to isotropize the CR distribution in the wave frame rather than the gas frame. When waves locally propagate in both directions, $\vec{u}_w$ represents an effective "compromise" drift frame for the CR and wave energies, which corresponds, in fact, to the motion of the "center of momentum" of the waves. The $\vec{u}_w$ terms directly alter the rate of CR acceleration by changing the speed at which CR are advected into and out of a shock structure and thus the rate at which the gas does work on the CR in a shock precursor. In passing I note that it is also convenient to term the condition $\nu_+ = \nu_-$ ($u_w = 0$; $v_A \neq 0$) an "isotropic" Alfvén wave field.

Solution of the full CR diffusion-advection equation [2.4] is numerically expensive and depends upon a number of physical, momentum dependent details that are not well understood (see, for example, Kang & Jones 1991, Duffy 1992). I will defer that more challenging problem to a subsequent paper. For an initial study of the most elementary Alfvén transport issues it is appropriate to use the simpler two-fluid approach instead, since it lends itself more easily to isolation of general dynamical issues. In that model equation [2.4] is multiplied by the kinetic energy of particles and integrated with respect to momentum. The resulting moments of f provide an energy conservation equation for the CR including finite Alfvén transport terms (*cf.* Achterberg 1982),

$$\frac{dE_c}{dt} = -\gamma_c E_c(\vec{\nabla}\cdot\vec{u}) + \vec{\nabla}\cdot(\langle\kappa\rangle\vec{\nabla}E_c - \vec{u}_w\gamma_c E_c) + \vec{u}_w\cdot\vec{\nabla}P_c + S, \qquad (2.8)$$

where E_c and $\gamma_c = 1 + P_c/E_c$ are the CR energy density and the ratio of specific heats, respectively, $\langle\kappa\rangle$ is an energy weighted, mean diffusion coefficient (*e.g.*, Kang, Jones & Ryu 1992), and for $\vec{u}_w$ I have set $h_w = 1$. The information absorbed into closure parameters in equation [2.8] prevent us from learning anything about momentum dependent evolution in a self-consistent way, but previous studies with $u_w = 0$ (*e.g.*, Kang and Jones 1991) have shown that within changes imposed from unmodeled variations in the values of γ_c and $\langle\kappa\rangle$ the resulting dynamical evolution is consistent with that obtained from the full diffusion-advection equation. Other concerns that have been raised about two-fluid models have to do with the fact that equation [2.8] does not explicitly keep track of the total number of CR particles (Jones & Ellison 1991), and that for very strong shocks where one expects $f(p)$ to become fairly flat so that $\gamma_c \rightarrow 4/3$, escape of the highest energy CR may prevent a true equilibrium from developing, even though one can find an equilibrium two-fluid solution. On the other hand, two-fluid models are purely dynamical models. Since the number of CR particles is expected to be relatively small, the only properties of any individual CR particle that matter are the energy and momentum that it carries. Only if any escaping particles begin to carry away significant fractions of E_c can they begin to alter the dynamics. That would require that $\gamma_c \approx 4/3$. But, as long as there is a significant admixture of nonrelativistic CR this will not be the case. Our own time dependent calculations with the full diffusion-advection equation (*e.g.* , Kang & Jones 1991) show that when the initial CR distribution is such that $\gamma_c > 4/3$, dynamical equilibrium is approached even though the CR particle distribution $f(p)$ may not reach an equilibrium, and before a sufficient number of particles are accelerated to such high energy that they might begin to alter the overall energetics or shock structure. Our purpose here is to explore the stages up

to dynamical equilibrium not to demonstrate the existence of a true particle equilibrium. Thus, those types of issues are not likely to influence results in the present paper. On longer timescales other issues such as the development of instabilities or the breakdown of planar geometry would seem to be at least as important (*e.g.* Jones & Kang 1992b).

In adding u_w to the two-fluid model I have introduced another degree of freedom with its own uncertainties, which clearly needs to be examined with extensions of the methods used in Kang & Jones (1991), before one can truly understand the quantitative nature of Alfvén transport. Remembering that our goals here are qualitative, and that the essential basic physics of the Alfvén transport is in equation [2.8], we expect to use these two-fluid results [2.8] as a standard for comparison and to provide direction for the more complete calculations, presently under development.

To close the system of equations we have the energy transport equation for the Alfvén wave fields in the WKB approximation according to Dewar (1970) (see also, Achterberg 1982).

$$\frac{dE_{wk\pm}}{dt} = -\sigma_{\pm}E_{wk\pm} \mp \vec{\nabla}\cdot(\hat{n}v_A E_{wk\pm}) - \frac{3}{2}E_{wk\pm}\vec{\nabla}\cdot\vec{u} - L_{k\pm}, \qquad (2.9)$$

where $-\sigma\pm$ is the energy growth rate of waves due to their resonant scattering with CR, and L_k is the dissipation rate for wave energy in the background plasma. Since the scales of interest greatly exceed the Larmour radii of thermal particles and the thickness of the subshock, other sources of wave growth at the appropriate wave numbers ought to be negligible within the shock (*e.g.* , Quest 1988). Other, nonlinear interactions such as wave-wave scatterings that lead indirectly through "nonlinear Landau damping" to wave dissipation can be incorporated into L_k (*e.g.* , VDM). For $\sigma_{\pm}$ I adopt the expression derived by Skilling (1975c) accounting for CR streaming in response to gradients in f and scattering by Alfvén waves propagating both parallel and antiparallel to $\hat{n}$; namely,

$$-\sigma_{\pm} = \frac{\pi^2}{3}\frac{m\Omega_o}{E_B}v_A\,\frac{p^3}{\nu_+ + \nu_-}\left[\mp v^2\hat{n}\cdot\vec{\nabla}f + 2v_A v(\nu_{\mp})\,(p\frac{\partial f}{\partial p})\right]. \qquad (2.10)$$

This shows the well-known feature that a CR density gradient stimulates growth of Alfvén waves propagating in the direction opposite to the gradient, but damps waves propagating into the gradient. Thus, in the precursor of a CR modified shock, the growing waves are propagating upstream. Steady CR modified plane shocks are uniform downstream of the shock transition, so no CR-generated wave growth or damping would result in the postshock flow. But, shocks evolving from a condition in which the CR pressure is smaller than the time asymptotic value will tend to generate CR distributions peaked around the shock. In that case it seems likely that amplification of Alfvén waves propagating downstream from the shock will result behind the transition.

Derivation of equation [2.8] was made much simpler by setting $h_w = 1$. This choice is consistent either with one of $E_{wk\pm}$ being dominant or with both wave fields having the same dependence on wavenumber. Comparable simplifications in the momentum average of equation [2.9] are available under similar conditions. Using equations [2.9, 2.10] we can begin to look at the plausibility of these situations. From equation [2.10] it is apparent

that when the incident wave field is small, streaming CR will tend to generate a field dominated by one of $E_{wk\pm}$. This was the rationale for Achterberg (1982) and McKenzie & Völk (1982) to use $\pm v_A$ for u_w. If, on the other hand, the incident wave field initially is isotropic, perhaps through nonlinear wave-wave equilibration, then according to equations [2.9 & 2.10] subsequent changes in $E_{wk\pm}$ will have similar k dependence, except possibly through $L_{k\pm}$. The specific Alfvén transport models described in §3 are all consistent with one or the other of these choices. In any case, our immediate goals are once again qualitative, and more complete calculations are underway to check the importance of such simplifications.

We can obtain total Alfvén wave energy conservation equations for the two directions, $E_{w\pm}$, by integrating equation [2.9] over wave number. If we again make the simplifying assumption that E_{wk+} and E_{wk-} have the same dependence on wave number, the ratio $\nu_\pm/(\nu_+ + \nu_-)$ can be taken outside the integral. This leads to the equation

$$\frac{dE_{w\pm}}{dt} = \frac{\mp\,\nu_\pm}{\nu_+ + \nu_-} v_A \hat{n}\cdot\vec{\nabla}P_c - \frac{2v_A^2}{c^2}\frac{\nu_\pm\langle\nu_\mp\rangle}{\nu_+ + \nu_-}(\gamma_c E_c) \mp \vec{\nabla}\cdot(\hat{n}v_A E_{w\pm}) - \frac{3}{2}E_{w\pm}\vec{\nabla}\cdot\vec{u} - L_\pm, \tag{2.11}$$

where $\langle\nu_\mp\rangle$ is averaged over wave number. The total Alfvén wave energy conservation equation is obtained by adding together both forms of equation [2.11] and using equation [2.5] to eliminate $\nu_\pm$ giving

$$\frac{dE_w}{dt} = -\vec{u}_w\cdot\vec{\nabla}P_c - \vec{\nabla}\cdot(\vec{u}_w E_w) - \frac{3}{2}E_w\vec{\nabla}\cdot\vec{u} - L, \tag{2.12}$$

where $E_w = E_{w+} + E_{w-}$, and $L = L_+ + L_-$. The second order term in (v_A/c) has been dropped. Of course, if one of $E_{wk\pm}$ dominates, equation [2.12] follows directly. Together with equations [2.1 - 2.3, 2.8] we now have a kind of three-fluid model for the plasma-CR-Alfvén wave system. Equation [2.12] is the same as that expressed by Achterberg (1982) or McKenzie and Völk (1982), except I have replaced v_A by u_w. In the models described below I will evaluate some consequences of using u_w instead of v_A.

The three separate energy conservation equations [2.2, 2.8, 2.12] combine to give the necessary relation for total energy conservation (*e.g.*, Achterberg 1982, McKenzie and Völk 1982)

$$\frac{\partial}{\partial t}(\rho e + E_c + E_w) + \vec{\nabla}\cdot\left[\vec{u}(\rho e + P_g) + (\vec{u}+\vec{u}_w)(\gamma_c E_c) - \kappa\vec{\nabla}E_c + (\frac{3}{2}\vec{u}+\vec{u}_w)E_w\right] = 0, \tag{2.13}$$

which explicitly displays the various contributions to the total energy flux in the system. It is clear, for example, how the total energy is influenced by the fact that CR and wave energy are advected differently from the gas energy.

3. SIMPLE MODELS

The equations of §2, supplemented by models for the microphysics of wave energy dissipation and CR injection, should allow one to solve for the evolution of CR modified

shocks including the evolution of the integrated Alfvén wave fields. Unfortunately, those microphysics models are not well established and even though they are idealized these equations are still very complicated and nonlinear. Thus, the present study will be restricted to some sets of still simplified models in order to anticipate better on what may be important to subsequent, more complete studies. We are now primarily concerned with evaluating the importance and properties of different aspects of Alfvén transport. Although I will allow the Alfvén speed to be significant with respect to other velocities in the problem, I will, as mentioned earlier, treat only parallel, sonic mode shocks, deferring the full, MHD, problem to later publications.

In the work to be described below the dynamical equations [2.1-2.3, 2.8, 2.12] have been solved numerically with an explicit, conservative hydrodynamics code based on the Piecewise Parabolic Method (Colella and Woodward 1984), augmented to include the Alfvén wave energy, plus a routine based on the implicit Crank-Nicholson scheme to solve the CR energy equation. The techniques are the same as those described in JK90 and Kang, Jones and Ryu (1992), except for the additional Alfvén transport terms. Tests of the code have been discussed previously (*e.g.*, JK90, Kang and Jones 1991, Kang, Jones and Ryu 1992). Some additional tests for the present extensions will be described in §4a below.

a) Initial Conditions

For this study I have simulated the evolution of 1D plane "shock tubes". The computational domain initially contains uniform left, (l), and right, (r), states, which in the absence of CR would generate steady, right facing gas shocks, moving relative to the upstream gas at speed, $u_s = 1.5$. Continuous boundaries exist on both ends of the grid. Initial gas state variables satisfy jump conditions for shocks of preselected sonic (gas) Mach numbers, $M = u_s/c_{sr} = 3$, 10 or 30, where c_{sr} is the upstream gas sound speed. For all the models discussed I assume upstream (right) states with $\rho_r = 1.0$ and $u_r = -0.5$, resulting in a nominal shock speed with respect to the "observer", $u_{so} = 1.0$. The initial P_c is uniform and everywhere equal to the upstream P_{gr}, so that $N = P_{cr}/(P_{cr} + P_{gr}) = 1/2$. The value of P_{gr} depends upon the selected sonic Mach number. I will not discuss models providing fresh injection of low energy CR; thus $S = Q = 0$. I have actually carried through a number of simulations in this study using an injection model described before (Kang & Jones 1990, JK90). However, since that particular feature does not appear to add any additional behaviors with regard to Alfvén transport questions, but increases the number of parameters, it seems appropriate to omit it for the time being. I consider here only models with constant γ_c. This should again be adequate for our present purposes. (See Achterberg *et al* 1984, Markiewicz *et al* 1990, Jones & Kang 1992b, Kang & Drury 1992, for discussions of the significance of that assumption.) For all except one model (Model 1 in Table 1) used to compare with results given in VDM, I have used $\gamma_c = 1.4$, which is approximately the value that would result from a power-law momentum distribution of the CR with index $q = 4.2$ (Achterberg, *et al* 1984). This is about the indicated form for galactic CR. Again, I have carried out other simulations with stiffer CR equations of state. No important qualitative differences from those discussed were apparent.

The Alfvén speed is determined by first defining its upstream value, v_{Ar}, in terms of the dimensionless parameter, β, given by

$$\beta = \left[\frac{c_{sr}}{v_{Ar}}\right]^2 = \frac{\gamma_g P_{gr}}{2E_B}. \tag{3.1}$$

Downstream and at all points after the simulations begin $v_A = \beta^{-1/2} c_{sr}\sqrt{\rho_r/\rho}$, reflecting the constancy and uniformity of the large scale magnetic field. The Alfvén Mach number of the shocks is $M_A = \beta^{1/2}M$. In order to avoid a variety of complications that can develop whenever $\beta < 1$, I will restrict the discussion to cases with $\beta \geq 1$. I set the initial upstream wave energy density $E_{wr} = \alpha E_B = \alpha\beta\rho_r c_{sr}^2/2$, where $\alpha \leq 1$ is a constant. The wave energy downstream of the *initial* shock discontinuity satisfies the relation $(E_w/\rho^{3/2})$ = constant; *i.e.*, the waves are assumed to have been adiabatically compressed through the initial jump (see equation[2.12]).

All the simulations discussed are based on a constant diffusion coefficient, $\langle\kappa\rangle = 0.35$. (For simplicity I will hereafter omit the brackets around κ.) This gives characteristic diffusion length and time scales, $x_d = \kappa/u_s = 0.233$, and $t_d = \kappa/u_s^2 = 0.156$, respectively. As pointed out previously (*e.g.*, Drury & Falle 1986), the width of the CR-generated shock precursor and the time scale for its evolution can be directly related to these scales. In fact, provided the dissipation rate, L, has an appropriate form such as that in equation [3.2] below, it is easy to see that the system of equations [2.1 - 2.3, 2.8, 2.12] can be written in dimensionless form by normalizing the length and time scales by x_d and t_d, the velocities by u_s or c_{sr}, densities by ρ_r and pressures and energy densities by $\rho_r c_{sr}^2$. The only necessary free parameters are then the dimensionless ratios N, M, β and α. Thus, we should concentrate on these dimensionless variables. Even if κ is not constant, one can formally write the dynamic equations in this way at the cost of burying an implicit dependence between κ and some other variables. Using a constant κ simplifies discussion and comparison of these models, since any differences in timescales of shock evolution are a direct consequence of Alfvén transport, rather than in the nominal diffusion timescale.

By assuming a constant κ for the models discussed I ignore the dependence between κ and E_w indicated through equation [2.7]. This simplification overlooks details in the structures and time histories of the shocks similar to those seen in earlier simulations involving density dependent κ, for example (JK90). However, the fact that the equations being solved can be written in a form not explicitly revealing κ suggests that in the normalized units above the general properties of the shock evolution should not depend significantly upon this decision. This outcome was previously demonstrated for the simpler cases without Alfvén transport (Drury and Falle 1986, JK90). To test this idea with Alfvén transport incorporated I did carry out one set of three shock simulations for the case $M = 10$, $\beta = 1$ and $\alpha = 0.5$, comparing the solutions with $\kappa = constant$, $\kappa \propto 1/\rho$ and $\kappa \propto 1/E_w$. (Otherwise these models were identical to Model 3 in Table 1). The detailed shock profiles and rates of evolution differed from each other in ways that one would anticipate (see, *e.g.*, JK90). But the differences at intermediate times were relatively minor and the time asymptotic post-shock states agreed exactly in all three cases to within tolerances expected from numerical convergence properties of the code (see §4a). Thus, I

believe the simplifications made by letting $\kappa = constant$ for the models described have not reduced the reliability of the conclusions reached. The behavior of the three models just described will be published elsewhere (Jones 1993).

b) Wave Dissipation and Streaming

To completely specify these models we still need to define properties for L and u_w. Although the microphysical details needed to do this in fully consistent ways are not well understood (see, *e.g.* VDM, Eichler 1985, Collins 1992 for some of the issues), my present purposes are exploratory, so that it is perhaps more useful to consider a simple range of possibilities. Thus, for the Alfvén wave dissipation rate, L, I will consider two idealized cases. For the first, I adopt the assumption by several previous authors (*e.g.*, VDM; Markiewicz *et al* 1990; Dorfi 1991) that dissipation of Alfvén waves within the plasma is in local equilibrium with the energy input from the CR; *i.e.*, so that the first and last righthand terms in equation [2.12] cancel. Then

$$L = -\vec{u}_w \cdot \vec{\nabla} P_c. \tag{3.2}$$

I will label this case "**LE**" (for local equilibrium) in Table 1. Note for this model that if $\alpha = 0$ initially, $dE_w/dt = 0$, and $\alpha = 0$ at all times. The second obvious, idealized alternative is to ignore Alfvén wave dissipation altogether, so that $L = 0$, which I designate by "**L0**".

For the streaming velocity, $\vec{u}_w$ I consider three simple models. Two of these assume $|\vec{u}_w| = v_A$. The first, following McKenzie & Völk 1982 and VDM, everywhere sets $u_w = v_A \geq 0$ (I designate this by "MV"), while the second sets the sign of $\vec{u}_w$ at a given location so that $\vec{u}_w \cdot \vec{\nabla} P_c \leq 0$. (This is designated "**UA**" in the model descriptors in Table 1.) Both of these models imply that Alfvén waves propagate locally in only one direction, so that the wave field is "fully anisotropic". The first model, MV, assumes that everywhere Alfvén waves propagate upstream. In front of the shock that is clearly anticipated by the argument that CR streaming upstream from the shock will amplify Alfvén waves propagating in the same direction. Downstream of the shock this expectation comes from the realization, both theoretically and observationally, that Alfvén waves generated by ions streaming upstream of parallel shocks in the heliosphere are swept back through those shocks and provide a fairly wide region of postshock MHD turbulence (*e.g.* , Quest 1988, Greenstadt 1985). On the other hand, for waves interacting with the more energetic particles of interest here this is a less obvious outcome, especially during time intervals that P_c is peaked around the shock. Then the same wave growth arguments used upstream should generate Alfvén waves propagating downstream behind the shock and damp waves in this region that propagate upstream. Wave fields reflecting that last property are represented most simply in the transport model UA.

The third $\vec{u}_w$ model is introduced to explore the possible importance of smooth variations in Alfvén wave isotropy within the flow, but away from the gas subshock, and to perhaps account more realistically for the competition between upstream facing and downstream facing waves in the postshock flow. This model assumes isotropic Alfvén

waves upstream of the shock precursor, *i.e.*, $E_{w+} = E_{w-}$, so that $u_w = 0$. But, in response to the streaming CR in the shock structure, $E_{w\pm}$ evolve differently to reflect their different responses to the CR; in particular, one of $E_{w\pm}$ should be amplified, while the other is damped. Thus we will expect u_w to grow within the precursor. Equations [2.11, 2.12] provide the means to determine $d(E_{w+} - E_{w-})/dt$ and du_w/dt. In general this will be complex and nonlinear, however. For present purposes it should be sufficient to adopt a behavior for u_w that is qualitatively similar to what we might expect in a more detailed treatment. To construct such a simple model for u_w I note that in the upstream region where $E_{w+} \approx E_{w-}$ and the rate of compression is still small, we have

$$\frac{d(E_{w+} - E_{w-})}{dt} \approx -v_A \hat{n} \cdot \vec{\nabla} P_c, \tag{3.3}$$

provided $L_+ \approx L_-$. Under these circumstances $u_w \propto (E_{w+} - E_{w-})/(\alpha E_B)$ exhibits linear growth. As the wave field anisotropy grows, however, u_w must become limited to v_A. The simplest model for u_w that has these qualities is

$$\frac{du_w}{dt} = \frac{1}{\tau}(\pm v_A - u_w) \tag{3.4}$$

whenever $|\nabla P_c| > 0$, or in practice when this gradient exceeds values produced by numerical round-off. The solution for u_w in equation [3.4] exponentially approaches $\pm v_A$, of course. The lower sign in equation [3.4] is meant to be applied within the postshock flow, where $\nabla P_c \geq 0$. Direct translation of equation [3.3] would give (see also Bell 1978, equation [20])

$$\tau \sim t_d \; M_A \frac{\alpha E_B}{P_c} \; \sim t_d M_A \frac{\alpha}{\beta} \frac{\rho c_s^2}{P_c}, \tag{3.5}$$

where $M_A = u_s/v_A$ is the Alfvénic Mach number of the shock. For the model parameters I have used $\tau \sim few \times t_d$. The advection time through the shock is of the order t_d, also. Although τ should vary in relation to t_d, it is sufficient for our immediate exploratory purposes to set τ/t_d to a constant of order unity. For the simulations discussed here, I arbitrarily set $\tau = 3t_d$. In Table 1 I will designate this class of transport model by "UE". I emphasize that the most important feature of this transport model is that u_w evolves smoothly towards the locally appropriate limit in response to $\vec{\nabla} P_c$.

In several simulations of CR acceleration in supernova remnants (Markiewicz *et al* 1990, Dorfi 1991) Alfvén transport was modeled exclusively in terms of the effects of wave energy dissipation; *i.e.*, terms resembling $|\vec{u}_w \cdot \vec{\nabla} P_c|$ were incorporated into the gas energy equation (equation [2.2]) and the CR energy equation, (equation [2.8]). Thus, as a final transport model, designated "D" in Table 1, I follow the same approach and drop all Alfvén advection terms and keep only the dissipative ones. The resulting calculations accounted for the excess generation of gas entropy within a shock precursor as a consequence of Alfvén wave damping. Markiewicz *et al* (1990) and Dorfi (1991) demonstrated that this can significantly change the evolution of a supernova remnant shock by increasing the postshock gas pressure and simultaneously decreasing the postshock CR pressure. Note that the two dissipative terms cancel in the total energy conservation equation [2.13], so this formalism appears at first to be internally consistent. However, it neglects the additional

flux term $\vec{\nabla} \cdot \vec{u}_w \gamma_c E_c$ in equation [2.8], which represents the fact that CR enthalpy is not advected at the same speed as the gas. Since that relative streaming changes across the shock in most circumstances, it also can be a very significant effect, and should be included for physical consistency (see, equation [2.13]). I note also that Markiewicz *et al* (1990) ignored Alfvén dissipative terms in the postshock region as one would expect for uniform conditions in an equilibrium shock, or when $u_w = 0$. However, since unsteady shocks will generally not offer uniform P_c downstream, and since the resulting gradients may generate streaming Alfvén waves, I will in model D include Alfvén dissipation on both sides of the shock, whenever ∇P_c is nonvanishing.

4. NUMERICAL RESULTS

Table 1 summarizes a sample of Alfvén transport model shocks whose evolution I have computed and will describe below. Columns 1 and 2 list the model number and the model type (§3b), column 3 gives the initial gas Mach number of the shock, M, while columns 4 and 5 list the magnetic field and Alfvén wave energy parameters, β and α. In addition to the models explicitly listed in Table 1, I have carried out for each value of M a comparison calculation in which $\beta \rightarrow \infty$; *i.e.* in which Alfvén transport is absent. Those models are, therefore, similar to ones discussed in JK90, and provide the means to establish the net consequences of Alfvén transport effects. I term these the "control" models, and refer to them specifically in the discussion as Models 3c, 6c and 7c. For most of the simulations discussed a uniform spatial resolution, $\Delta x = 0.0146$, was used; for Model 10 ($M = 30$) $\Delta x = 0.0098$. Except for Models 7 and 8, the spatial interval was [0, 120]. In those two models ($M = 3$) it was [0,60]. The initial discontinuity was placed at x = 9.375 to be far enough away from the two boundaries, so that $\nabla P_c = 0$ there at all times. Simulations were carried out from $t = 0$ until $t = 110$ ($t/t_d \approx 700$), except for Models 7 and 8, for which the final $t = 30$ ($t/t_d \approx 200$). This was long enough for most of the simulations to approach a steady state in the region within and immediately behind the shock.

a) Tests

Since we need to compare a variety of subtle effects it is important to understand the accuracy of the numerical results. I have explored this in several ways. The first was to perform a simple test for convergence to a final steady state in each model. In a steady state the upstream and downstream mass fluxes (ρu) and momentum fluxes ($\rho u^2 + P_g + P_c + P_w$) measured in the shock frame should be conserved. (Of course, the time dependent versions of these conservation laws are always exactly satisfied in the computations.) It is not possible to determine the exact final shock speed or Mach number *a priori*, because it depends upon P_c in the shock structure, which, itself depends on the shock speed. Thus, assuming the constancy of mass flux to define a suitable shock speed, I tested the second conservation law. At the end of each control model simulation and most of the others I found that the upstream and downstream momentum fluxes agreed to within about 1 - 2 %, using the resolutions listed above. This, therefore, represents an approximate estimate of our ability to discriminate effects on individual components to the momentum flux in the asymptotic limit. As a second step I tested the final convergence of

the control models to exact steady solutions as defined in Drury & Völk (1981) and Kang & Jones (1990). In each case I found exact steady solutions whose densities, velocities and momentum fluxes in the shock frame all agree to within about 2% of the final numerically determined states using the resolutions listed above. The individual asymptotic postshock values of P_c and P_g are likewise consistent, with an accuracy $\sim$ 2% in terms of the total momentum flux. Previously we have established (JK90) that convergence for CR shocks as measured above is limited by the degree to which the shock precursor (width $\sim x_d$) is resolved in the computation. The numerical resolutions above correspond to $x_d/\Delta x \approx 16$ and 24, similar to values we have incorporated in our earlier work.

To test specifically for convergence to accurate solutions including Alfvén transport, I computed one model whose exact steady solution was given by VDM. This is Model 1 in my Table 1, and its steady solution can be found by using Figure 1 in VDM. To make the comparison properly one must first convert the gas Mach number used here ($M = 10$) to the generalized Mach number used by VDM. That can be done with their equation [B8] after correcting an obvious typo. In their units the Mach number is 5.9. Figure 1 here shows the comparison with values estimated from their graph. The agreement between the final numerical postshock state and the VDM solution is comparable to the measures cited above. As a final code test I have carried out the computation of several of the models in Table 1 with both of the resolutions listed above and found them to differ at all times and locations by much less than the uncertainties defined through the other tests described. Thus, in summary, I feel confident that the solutions being presented are accurate to the level of a couple of percent or better of the bulk flow properties.

b) Alfvén Transport Results

Some of the general consequences of Alfvén transport can be seen by examining Figure 2, which displays structures near the end of the simulations of Models 2-4 (all with $M = 10, \beta = 1$ and $\alpha = 0$). The $M = 10$ control, Model, 3c, is also shown at a somewhat earlier time, but still in a converged state. The qualitative time histories of all the models are similar to those described in JK90 and Kang & Jones (1991), so I will concentrate here on their differences. Two important things are immediately clear from the figure. First, Alfvén transport in each of Models 2-4 has an important effect on the final as well as the intermediate shock structures. (Those intermediate properties are preserved in the flow profiles shown.) In each case it has reduced P_c below levels seen in the control Model 3c, and has left the postshock gas hotter. For these parameters the gas subshock is still present, but considerably weakened in the control model. In all the models incorporating Alfvén transport, the gas subshock is strong, even approaching the original strength in one case (Model 3). The second point is, however, that the impact of Alfvén transport depends strongly upon the details of how it is modeled. This is obvious in the P_c and P_g profiles in the figure. In addition, since P_c softens the equation of state of the fluid in the shock relative to that from P_g alone, the differing postshock values of P_c result in slight variations in the shock speed as well as more significant differences in the postshock gas density. The large overcompressed density features visible in Models 3c and 2 are absent in Models 3 and 4. That is due directly to their smaller P_c, as discussed previously (JK90).

Model 2 is based on the Alfvén transport model described in VDM. Among the models shown in Figure 2 it produces the least change in CR acceleration efficiency compared to the control model; *i.e.*, it generates the greatest postshock P_c, next to the control model. Model 3 produces the most change; the smallest P_c and largest P_g. Models 2 and 3 differ in only one detail of the Alfvén transport *downstream* of the gas subshock, yet the asymptotic postshock values of P_c differ by a factor ≈ 7. The distinction between the models is the direction assumed for $\vec{u}_w$ in the postshock flow, as illustrated in the lower left portion of Figure 2. Both models assume that $|\vec{u}_w| = v_A$; however, Model 2 assumes that $\vec{u}_w$ always points upstream, whereas Model 3 reverses $\vec{u}_w$ to point downstream in the postshock flow, as discussed in §3b. Two important changes result from this distinction. First, $\vec{u}_w \cdot \vec{\nabla} P_c > 0$ in the postshock flow of Model 2 when P_c is building up. Then since Model 2 uses equation [3.2] to define the rate of Alfvén wave dissipation and consequent nonadiabatic gas heating outside the subshock, $L \leq 0$ in the postshock flow; *i.e.*, heat is removed from the gas and put into the CR. That particular feature of Model 2 is unphysical. But, even though it would seem to be irrelevant once the shock has reached a steady state with a uniform downstream condition, it does play a role in *getting to* the steady state.

The second distinction between Models 2 and 3 is more important and does remain a factor even in the steady state. This is the fact that the Alfvén wave advection through the fluid as represented by $\vec{u}_w$ changes the rate at which compression in the gas flow does work on the CR. That is related to the rate at which individual particles are accelerated as they scatter back and forth across the shock. In all the models discussed in this paper this rate is slower because of Alfvén wave advection, but the amount of change depends upon how $\vec{u}_w$ varies within the flow. In general the effects will be greater whenever M and β are smaller. We can evaluate this behavior simply using the formula for the mean time interval for a particle to be accelerated to some momentum $p + dp$ from an initial momentum p (Lagage & Cesarsky 1983, Drury 1983),

$$dt = \left(\frac{3}{\tilde{u}_1 - \tilde{u}_2}\right)\left(\frac{\kappa_1}{\tilde{u}_1} + \frac{\kappa_2}{\tilde{u}_2}\right)\frac{dp}{p}. \qquad (4.1)$$

The mean particle acceleration rate $\sim dp/dt$. In this equation the subscripts 1 and 2 refer to the upstream and downstream values of the diffusion coefficient, κ, and the net advection speed, $\tilde{u} = u + u_w$, as measured in the shock frame. The interval dt in equation [4.1] includes two velocity dependent effects, isolated by brackets. The first is the momentum change produced by a single reflection through the shock, $\delta p \propto \tilde{u}_1 - \tilde{u}_2$. Alfvén wave advection will always diminish δp, no matter what the direction of $\vec{u}_w$, provided $|u_{w1}| > |u_{w2}|$. This factor always tends to increase dt, therefore. The remaining part of dt comes from the mean residence time of a particle on each side of the shock, $t_{r1,2} \propto \kappa_{1,2}/\tilde{u}_{1,2}$. The residence time on the upstream side of the shock, t_{r1}, will always be increased, compared to a case without Alfvén transport by upstream directed Alfvén advection. It is the relative downstream residence time, t_{r2}, that most distinguishes Models 2 and 3, since it is decreased in Model 2 but increased in Model 3. However, for the models discussed here, $t_{r1} > t_{r2}$, so that in net dt is always increased by these changes. From this example we can see that the properties of Alfvén transport *behind* the shock are important to the rate of CR acceleration in the shock.

Models 3 and 4 allow us to see directly the relative roles of Alfvén wave dissipation and advection in diminishing CR acceleration. Model 4 differs from Model 3 only in having the Alfvén advection terms turned off. As discussed in §3b, this model resembles those used in some previous efforts to include Alfvén transport in models of supernova remnant CR acceleration. The simplification made reduces significantly the impact of Alfvén transport in this case. Model 4 has not quite reached a steady state at the end of the simulation, but, even so, it has generated a postshock P_c that is already ≈ 3.5 times greater than that in Model 3. The reasons for the difference are simply related to the fact that the elimination of Alfvén advection in Model 4 causes dt in equation [4.1] to be smaller in Model 4 than in Model 3. It is conceivable, of course, that nonlinear processes in the postshock flow might produce a more nearly isotropic Alfvén wave distribution, thereby reducing or eliminating postshock Alfvén advection. Then Model 4 would be a crude approximation to the expected behavior, although it would still overestimate the rate of particle acceleration, because it also ignores upstream Alfvén advection. In any case, it is clear that we must properly include the advective terms in Alfvén transport for an accurate model.

Model 5 is a simple attempt to illustrate the potential significance of a related detail; namely, the smooth spatial and temporal evolution of $\vec{u}_w$ through the full shock structure. As outlined in §3b, Model 5 allows $|u_w|$ to evolve relative to v_A in response to gradients in P_c. It is zero upstream of the shock, representing an assumed isotropy of the waves in that region. The resulting behavior can be compared to that of Model 3 using Figure 3. For Model 5 the Alfvén transport terms are effectively turned off upstream of the shock precursor. Furthermore, the sign change in u_w which is at the gas shock in Model 3 is delayed behind the shock while the relative balance of forward rate and reverse propagating Alfvén waves responds to damping and growth by the CR (see Figure 3). As we would anticipate from these features and what has already been stated, Model 5 is significantly more efficient in CR acceleration than Model 3. Since Model 5 has not yet reached an equilibrium we cannot say with certainty how large the time asymptotic P_c will be. At the end of the simulation it is still much smaller than the final value for Model 2, but it is plausible that Model 5 could ultimately approach this level of efficiency, albeit much later than Model 2. That suggestion follows from the recognition that in one important respect the Alfvén transport in Model 5 has begun to approach that in Model 2. By examining the evolution of u_w one can see that the region behind the subshock within which $u_w > 0$ has extended with time. In a more realistic model, the rate of change in u_w would depend on the size of ∇P_c, which has diminished with time, as well. That should cause the sign change in u_w to be further delayed downstream. Once the region with $u_w > 0$ extends more than a length $\sim \kappa/u2$ downstream from the shock, Models 2 and 5 should be qualitatively similar in terms of their Alfvén transport properties. An additional, curious feature of Model 5 comes from the fact that u_w develops finite values within the precursor in response to finite ∇P_c. This results in a nonlinear effect that causes the tip of the precursor in to extend forward at an enhanced rate, producing a kind of "toe", just visible in P_c in the figure. The foreshock region is consequently somewhat broader at its base than it would be otherwise.

So far we have examined only shocks of nominal Mach number 10. It has long been known that the efficiency of diffusive shock acceleration and the degree of shock modification due to back reaction from the CR depend upon the Mach number of the shocks involved (*e.g.,* Axford, Leer & Skadron 1977; Blandford 1980; Drury & Völk 1981). In general acceleration efficiency is highest and shock modification is greatest when the Mach number is high, at least in the time asymptotic limit. But, Alfvén transport complicates this issue, since it is itself nonlinear. The VDM model of Alfvén transport has a relatively modest effect on acceleration efficiency at both small and very large Mach numbers (see Figure 1 in VDM). The VDM Alfvén transport model has its greatest impact in moderately strong shocks, such as those already discussed. Our results already described confirm theirs, that at intermediate Mach number, Alfvén transport can be generally quite important. But, since the degree of change was so model dependent, it may be useful to compare the VDM results at greater and lesser Mach numbers to the behavior using other Alfvén transport models before drawing conclusions for shocks of different strengths. Figures 4 and 5 allow us to do this for cases $M = 30$ and $M = 3$ using the same Alfvén transport model as in the Mach 10 Model 3, discussed previously.

Figure 4, compares the evolution of two $M = 30$ shocks (Model 6 and the control, Model 6c). As emphasized earlier, diffusive shock acceleration models that do not incorporate Alfvén transport can be so efficient at transferring energy to CR in the time asymptotic limit that they completely smooth out the shock transition (eliminate the entropy producing gas subshock) at high Mach numbers. That does indeed happen in the control model shown in the figure. Such a development would have quite a significant impact on the observed properties of the gas in the postshock flow, since the gas will be significantly colder. The fact that X-rays are observed from behind supernova shocks, thus providing proof that these shocks are not smoothed out, has sometimes been cited as an indication that the theory of diffusive shock acceleration may overestimate real efficiencies. There are several ways that this issue can be ameliorated, including not assuming a steady state (see, *e.g.* Jones & Kang 1992a). But, as pointed out by VDM, one of the potentially most important consequences of Alfvén transport is that, by reducing the efficiency of CR acceleration in strong shocks, it might delay to much higher Mach number potential development of the smoothed out transition. That expectation is certainly borne out in Model 6, shown here. In fact the gas shock has retained almost its original strength even at Mach 30, with a postshock pressure ratio, $P_g/P_c > 10$. This is once again a significantly greater diminution of the CR acceleration efficiency than with the VDM transport model. They estimated with their model for $\gamma_c = 4/3$ and $N = 1/2$ that Alfvén transport would extend the range of gas Mach numbers for which subshocks are expected to ~ 50 (or ~ 30 in their Mach units) when $\beta = 1$. The result shown here supports that suggestion.

On the other end of the Mach scale, Figure 5 illustrates the time evolution of the $M = 3$, Model 7 shock, which once again uses the same Alfvén transport as in Model 3. The Mach 3 control, Model 7c is also shown, along with the ending state for the analogous Model 8 which uses an intermediate $\beta = 10$. It is clear that the Alfvén transport effects are quite significant even at Mach 3 in this case. The asymptotic postshock value of P_c is decreased in Model 7 relative to Model 7c by a factor of ≈ 4.2. That impact of Alfvén transport appears to be much greater than in the VDM model, because, once again Alfvén

wave advection behind the shock influences the rate of particle acceleration. The potential importance of that advective effect and sensitivity of results to the way Alfvén advection is modeled will become greater as the difference between v_A and the postshock gas speed, u_2, diminishes. It is straightforward to show in the absence of CR modification to the flow that the ratio $v_A/u_2 = \sqrt{(\gamma+1)/\left\{\left[(\gamma-1)M^2+2\right]\beta\right\}}$ which is a monotonically decreasing function of M. Note, however, that so long as $\beta \geq 1$ and $M > 1$, then $v_A/u_2 < 1$, so that we avoid such complicating developments as "switch-on" shocks, wherein the postshock flow develops a large scale magnetic field component tangent to the shock face. The ending state of Model 8 with $\beta = 10$ is shown to demonstrate that at such low Mach numbers Alfvén transport can still be significant, even when the magnetic field is not all that strong. The ending P_c in Model 8 is still only about 2/3 the asymptotic value in Model 7c. An analogous comparison between the Mach 10 control Model 3c and a like example with $\beta = 10$, produces less than 20% difference in the final, asymptotic P_c.

Finally, Figure 6 illustrates the evolution of two $M = 10, \beta = 1$ models (Models 9 and 10) for which the finite Alfvén wave energy, E_w, has been explicitly accounted for in the dynamics. In particular, they represent cases in which $\alpha = 1$. Model 9 is identical to Model 3, except for that feature. A comparison between the evolution of those two models (using Figures 3 and 6, for example) shows that in this case, at least, the addition of the wave energy has little impact on the behavior. The forces resulting from P_w are never very large compared to the dominant terms, so this is not very surprising. Even though the nonlinear processes which might limit E_w are not well established, there should be general agreement that $\alpha = 1$ is a conservative upper limit to what might be expected. In fact, since the downstream E_w/E_B is increased, this is perhaps too large to be entirely consistent with the spirit of the models. Thus, for parallel shocks with $\beta \geq 1$, at least, it seems that the Alfvén wave energy should not be *directly* important to the dynamics. We assumed above a local equilibrium in wave energy gains from CR and dissipation in the gas. So E_w does not increase substantially above levels based on adiabatic compression used as initial conditions. Because a local equilibrium ("LE") may not be wholly realistic, one might reasonably ask how sensitive the previous behavior was to that assumption. Model 10, also shown in the figure, may provide a partial answer to that question, since it is identical to Model 9 except it assumes there is *no* wave dissipation; *i.e.*, that $L = 0$. This clearly makes quite a difference, since P_c is still growing almost linearly in time even at the end of that simulation and is considerably greater than the equilibrium value in Model 9. However, the effect on the wave growth itself is less dramatic, since it is only $\sim 20\%$ larger at the end of the simulation than it was in Model 9. Most of the difference in the two outcomes must be due to the fact that the gas remains colder in Model 10 and compression is greater, so that energy gains by particles crossing the subshock are greater. Note that in Model 10 Alfvén advection remains in effect and that $\vec{u}_w \cdot \vec{\nabla} P_c$ remains in place in equation [2.8], so that only the gas and wave energy equations have been influenced. The influence of Alfvén advection may account for the greater time scale apparently required for the shock in Model 10 to approach an equilibrium. That is, as discussed earlier, particle residence times on each side of the subshock are extended by Alfvén advection. It is clear from this example that the details of the wave damping model can be important, even if the wave energy content itself is not large enough to impact directly on the flows.

5. SUMMARY

This paper has explored the time evolution of plane, cosmic-ray modified parallel shocks based on the diffusive shock acceleration formalism and including the effects from the finite propagation speed and energy of Alfvén waves responsible for controlling the transport of the cosmic-rays. The numerical simulations discussed are based on a three-fluid model for the dynamics. The results of the simulations confirm earlier, steady state analyses that found these Alfvén transport effects to be potentially important when the upstream Alfvén speed and gas sound speed are comparable. It is also apparent, however, that the impact of Alfvén transport effects under such conditions, which tend to slow shock evolution and reduce the time asymptotic cosmic-ray pressure in the shock, is strongly dependent upon details of the transport. It is clear that both cosmic-ray advection tied to streaming Alfvén waves and dissipation of wave energy are important to include in the models. It was obvious from the start, of course, that Alfvén transport should not play a very important role if the magnetic field is weak in the sense that the Alfvén speed is negligible. However, what constitutes a negligible Alfvén speed in terms of the gas sound speed or the shock speed also seems to depend significantly on the transport characteristics.

The influence of Alfvén transport depends upon both direct advection through the underlying plasma brought about by streaming of Alfvén waves and by the dissipation of the wave energy generated through the resonant scattering between waves and cosmic-rays. Alfvén advection, used here to refer to the direct transport of cosmic rays in the "center of momentum" frame of the Alfvén waves is important, because, by changing the relative speeds of the "mirrors" across the shock, it alters the energy gained each time a particle crosses the shock. In addition Alfvén advection can extend or decrease the characteristic time spent by an energetic particle before it returns across the shock, thus further modifying the rate of acceleration. Wave dissipation is important not only because it represents direct energy removal from the cosmic rays, but also because it can influence the compression in the shock, and thus the energy gain by a particle in each shock crossing.

Although the general consequences of Alfvén transport are to slow down the rate of cosmic ray acceleration and to reduce the available efficiency of the process, how significant the effects are is rather sensitive to a number of details, currently not well understood, about the generation, propagation and dissipation of the Alfvén waves in these environments. Depending upon these details it would appear under some circumstances that Alfvén transport can dramatically retard and/or reduce the efficiency of diffusive shock acceleration. But relatively simple changes in the Alfvén transport characteristics can considerably alter the predicted acceleration efficiency. These statements refer both to the time asymptotic state of the shock and to its intermediate structures. The simulations reported here demonstrate, for example, that the variation of the streaming motion of the Alfvén waves through the shock structure can be very important and influence such basic matters as the net efficiency of acceleration at a given time, the time necessary to reach an equilibrium and the range of Mach numbers over which one might expect eventually to have the shock structure smoothed out by back reaction of the cosmic rays. Along the same lines, it is clear from these calculations that the properties of Alfvén transport on

both sides of the shock transition should be carefully considered in evaluating its influence on diffusive shock acceleration.

These calculations were intended primarily to help establish directions for developing more complete treatments of Alfvén transport in diffusive acceleration shock models. They are still very idealized and clearly do not provide a full picture of the problem. The results do indicate that one must carefully consider the details of such models, and that further efforts are needed to refine our physical understanding of Alfvén transport. It is also clear that before we can be at all confident we understand what role, if any of practical importance, Alfvén transport plays in real astrophysical shocks, we must extend such treatments as this one to include full MHD as well as momentum dependent aspects of the problem. The structures of oblique MHD shocks can be more complicated than those considered here, especially when the magnetic fields are strong. Further, in an oblique field geometry the Alfvén advection, which is along the field lines, will not transport cosmic rays so rapidly with respect to the shock boundary. Other important, field related details of acceleration physics may also enter the picture (*e.g.* , Jokipii 1992). In a two-fluid or three-fluid model, we cannot consider such effects as the different rates of scattering and wave growth appropriate to different momentum ranges of the particles. Since the scattering rates and wave growth rates may reasonably be slower for large momenta, this could mean, for example, that for the high energy particles that are directly observed, Alfvén transport effects are diminished relative to those for the lower energy particles that are most likely to become involved in nonlinear back reaction on the shock flow.

Acknowledgments

This work was supported in part by NASA through grant NAGW-2548, the NSF through grant AST-9100486, and by the University of Minnesota Supercomputer Institute. I am very grateful to Hyesung Kang for valuable discussions, comments on the manuscript and, especially, for her contributions to previous studies which made this work possible. I also thank Larry Rudnick and an anonymous referee for constructive comments and Paul Woodward, for providing me with the original PPM hydrodynamics code from which that used here has been developed. The MSI generously extended hospitality while this work was carried out.

TABLE 1

Alfvén Transport Model Shock Properties[1]

Model	Transport Properties[2]	M	β	α
1	LE-MV	10	5/6	0.
2	LE-MV	10	1	0.
3	LE-UA	10	1	0.
4	LE-UA-D	10	1	0.
5	LE-UE	10	1	0.
6	LE-UA	30	1	0.
7	LE-UA	3	1	0.
8	LE-UA	3	10	0.
9	LE-UA	10	1	1
10	L0-UA	10	1	1

[1] All models have $N = 1/2$ and $\gamma_g = 5/3$.

All models except model 1 have $\gamma_c = 1.4$. For model 1 $\gamma_c = 4/3$.

[2] See §3b.

REFERENCES

Achterberg, A. 1982, A&A, 98, 195.

Achterberg, A., Blandford, R.D. & Periwal, V. 1984, A&A, 132, 97.

Axford, W. I., Leer, E. & Skadron, G. 1977, Proc. 15th International Cosmic Ray Conference (Plovdiv), 11, 132.

Bell. A. R. 1978, MNRAS, 182, 147.

Blandford, R. D. 1980, ApJ, 238, 410.

Blandford, R. D., & Eichler, D. 1987, Phys Rept, 154, 1.

Chin. Y. & Wentzel, D. G. 1972, Ap & Space Sci., 16, 465.

Colella, P., & Woodward, P. R. 1984, J Comp Phys, 54, 174.

Collins. W. 1992, ApJ, 384, 319.

Dewar, R. L. 1970, Phys. Fluids, 13, 2710.

Dorfi, E. A. 1991 , A& A, 251, 597.

Drury, L. O'C. 1983, Rept Prog Phys, 46, 973.

Drury, L. O'C. & Falle, S. A. E. G. 1986, MNRAS, 223, 353.

Drury, L. O'C., & Völk, H. J. 1981, ApJ, 248, 344.

Duffy, P. 1992, A&A, 262, 281.

Eichler, D. 1985, ApJ, 294, 40.

Ferrière, K. M., Zweibel, E. G., & Shull, M. J. 1988, ApJ, 332, 984.

Greenstadt, E. W. 1985, in *Collisionless Shocks in the Heliosphere:Reviews of Current Research*, ed. B. T. Tsurutani & R. G. Stone (Washington: American Geophysical Union), p.169.

Jokipii, J. R. 1992, in *Particle Acceleration in Cosmic Plasmas*, ed. G.P. Zank & T. K. Gaisser (New York: American Institute of Physics), p.137.

Jones, F. C., & Ellison, D. C. 1991, Space Sci. Rev., 58, 259.

Jones, T. W. 1993, IAU Colloquium 142, to be submitted.

Jones, T. W., & Kang, H. 1990, ApJ, 363, 499 (JK90).

Jones, T. W., & Kang, H. 1992a, in *Particle Acceleration in Cosmic Plasmas*, ed. G.P. Zank & T. K. Gaisser (New York: American Institute of Physics), p.148.

Jones, T. W., & Kang, H. 1992b, ApJ, 396, 586.

Jones, T. W., & Kang, H. 1993, ApJ, 402, 560.

Kang, H. & Drury, L. O'C. 1992, ApJ, 399, 182.

Kang, H., & Jones, T. W. 1990, ApJ, 353, 149).

Kang, H., & Jones, T. W. 1991, MNRAS, 249, 439.

Kang, H., Jones, T. W., & Ryu, D. 1992, ApJ, 385, 193.

Lagage, P. O. & Cesarsky, C. J. 1983, A&A, 125, 249.

Lee, M. A. 1983, JGR, 88, 6109.

Markiewicz, W. J., Drury, L. O'C., & Völk, H. J. 1990, A& A, 236, 487.

McKenzie, J. F. & Völk, H. J. 1982, A&A, 116, 191.

Quest, K. B. 1988, JGR, 93, 9649.

Schlickeiser, R. 1992a, in *Particle Acceleration in Cosmic Plasmas*, ed. G.P. Zank & T. K. Gaisser (New York: American Institute of Physics), p.92.

Skilling, J. 1975a, MNRAS, 172, 557.

Skilling, J. 1975b, MNRAS, 173, 245.

Skilling, J. 1975c, MNRAS, 173, 255.

Spitzer, L. 1978, *Physical Processes in the Interstellar Medium* (New York: John Wiley & Sons).

Völk, H. J., Drury, L. O'C., & McKenzie, J. F. 1984, A&A, 130, 19 (VDM).

FIGURE CAPTIONS

Fig. 1.— Evolution of a plane cosmic-ray modified shock including Alfvén transport effects according to a transport model by Völk, Drury and McKenzie (1984) and described here in §3b. Shock properties are listed as Model 1 in Table 1. The solid curves, representing gas density, pressure and velocity along with the cosmic ray pressure are structures numerically determined from time dependent techniques described in the text and shown at times $t = 0, 50, 110$. For all models in all figures the characteristic diffusion time is $t_d = \kappa/u_s^2 = 0.156$. The dashed lines are values taken from the exact steady state solution for this shock as given in Figure 1 of Völk, *et al.* .

Fig. 2.— Ending cosmic-ray modified shock structures for Models 2, 3 and 4 as described in the text and listed in Table 1. The control Model 3c, without Alfvén transport effects, is also shown. Models are labeled in the upper right panel. Structures for Models 2, 3 and 4 are shown at $t = 100$, while Model 3c is shown at $t = 70$. u_w is the mean drift speed of the Alfvén waves through the background plasma. The solid curves represent initial conditions ($t = 0$) for the models. The small cusps in the density profiles in this and the other figures occur in the Lagrangian sense at the original shock location and result from the nonequilibrium nature of the assumed shock initial conditions.

Fig. 3. — Computed shock structures for Models 3 (solid) and 5 (dotted) from Table 1. Structures are shown at $t = 0, 30, 60, 90$.

Fig. 4.— Shock structures for Models 6 (dotted) and 6c (solid) at times $t = 0, 30, 60, 90$.

Fig. 5.— Shock structures for Models 7 (solid) and 7c (dotted) at times $t = 0, 10, 20, 30$. Also shown is the structure of Model 8 (dashed) at $t = 30$.

Fig. 6.— Shock structures for Models 9 (dotted) and 10 (solid) at $t = 0, 30, 60, 90$.

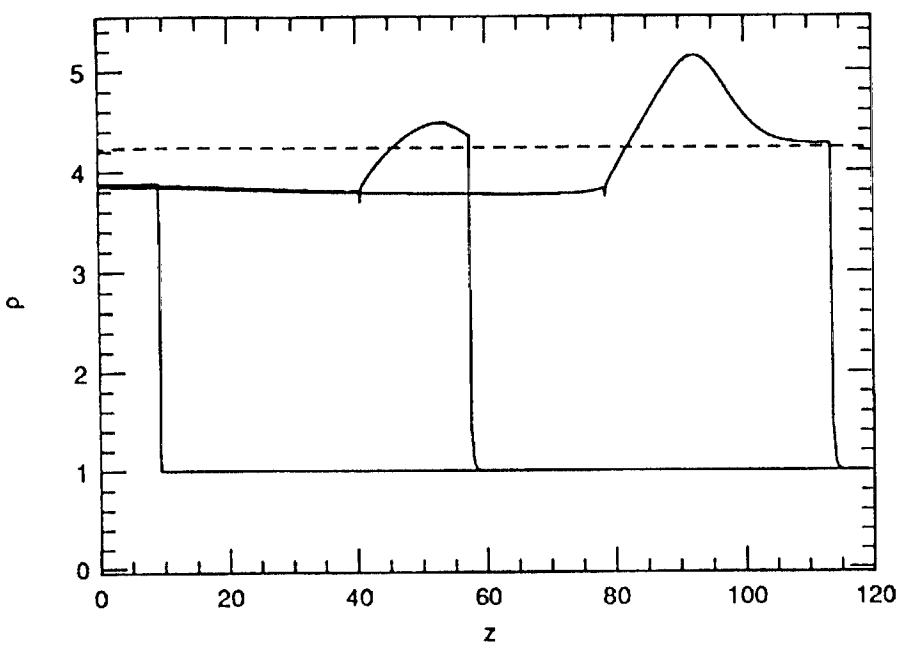
ρ
z
0
1
2
3
4
5
0
20
40
60
80
100
120

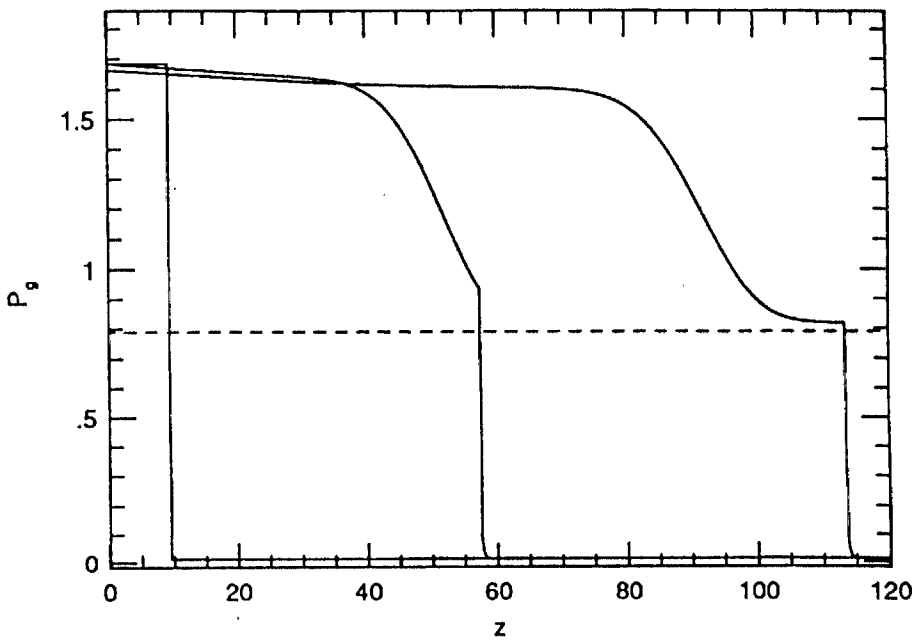
P_g
z
0
.5
1
1.5
0
20
40
60
80
100
120

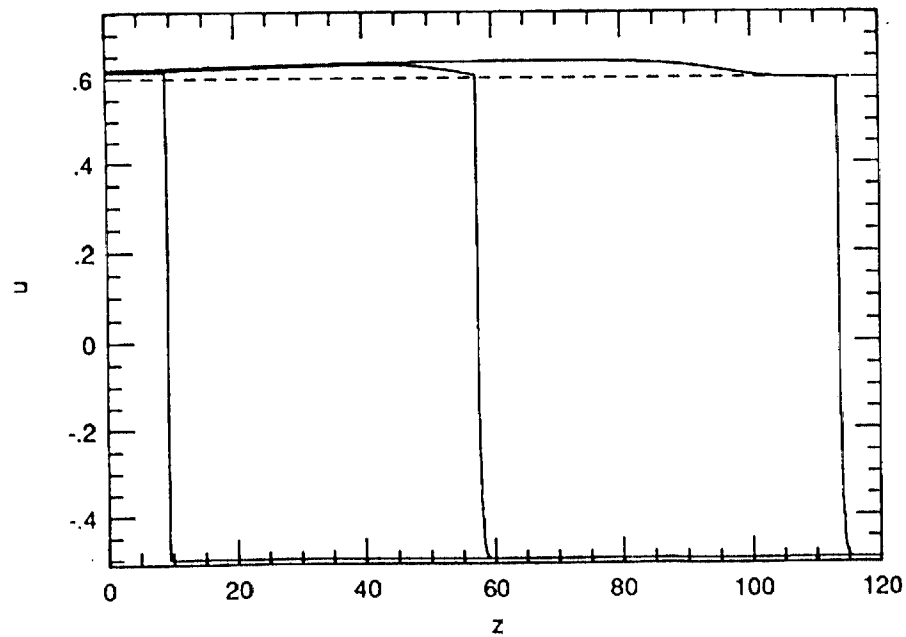
u
z
-.4
-.2
0
.2
.4
.6
0
20
40
60
80
100
120

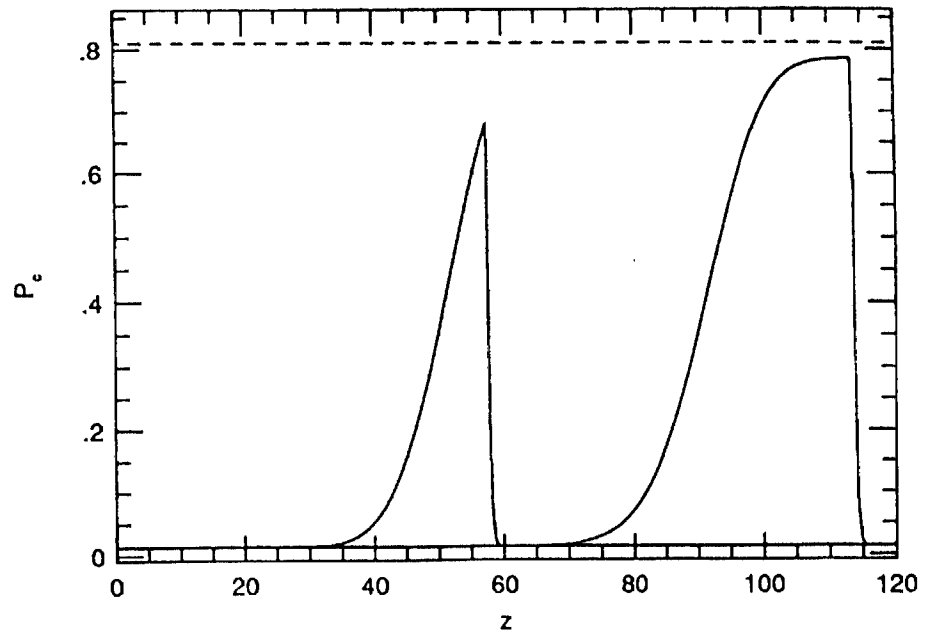
P_e
z
0
.2
.4
.6
.8
0
20
40
60
80
100
120

Fig 1

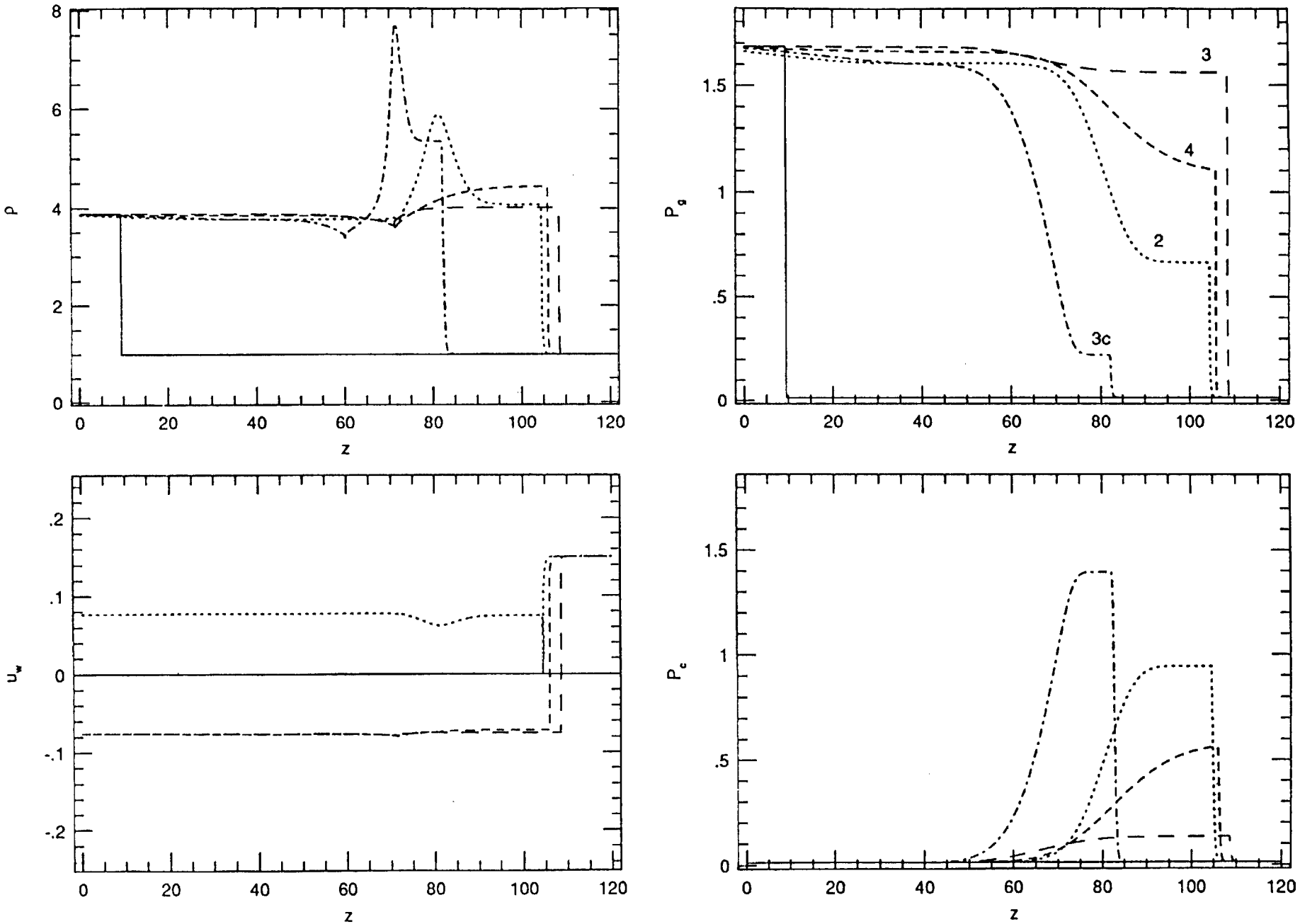

Fig 2

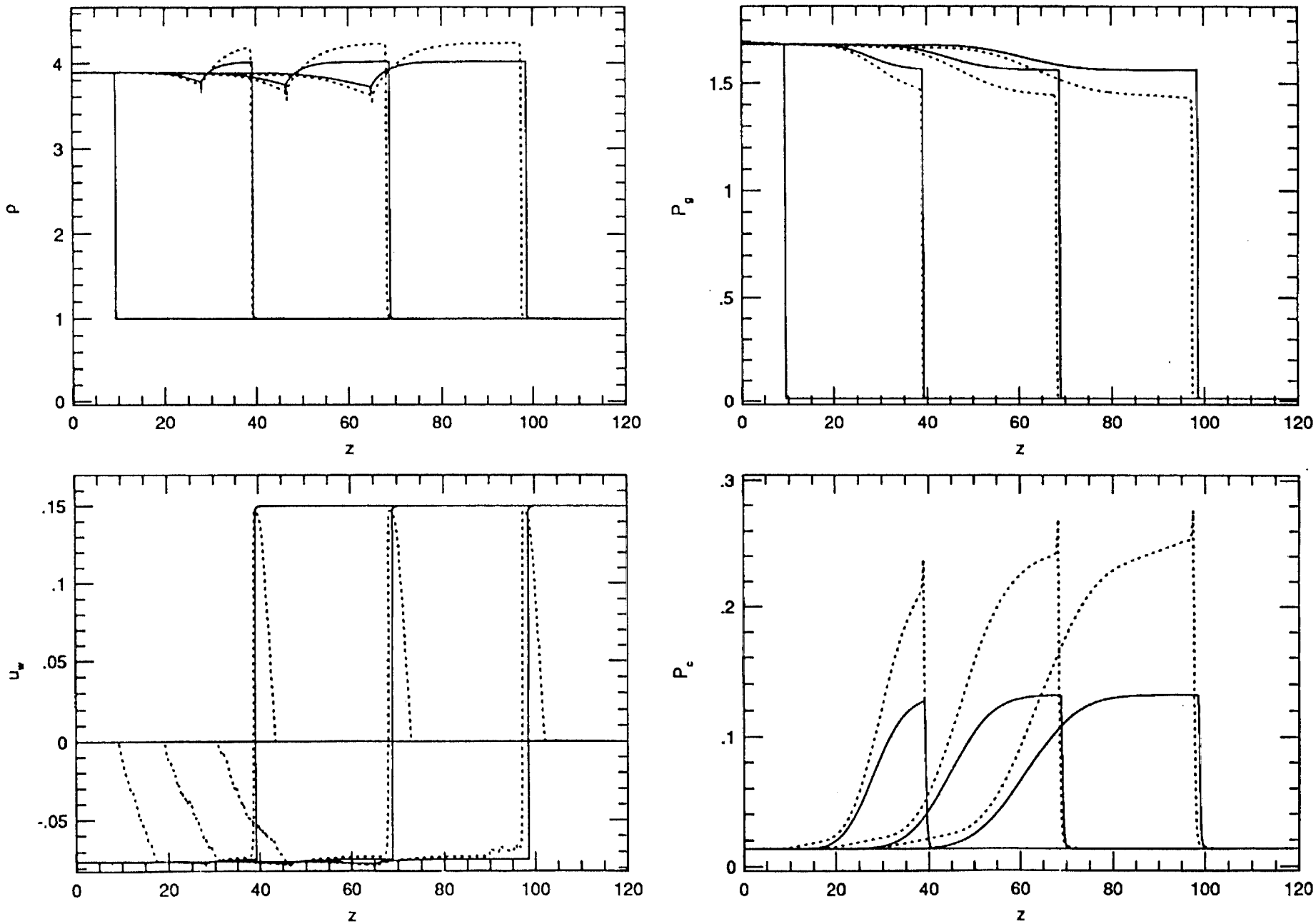

Fig3

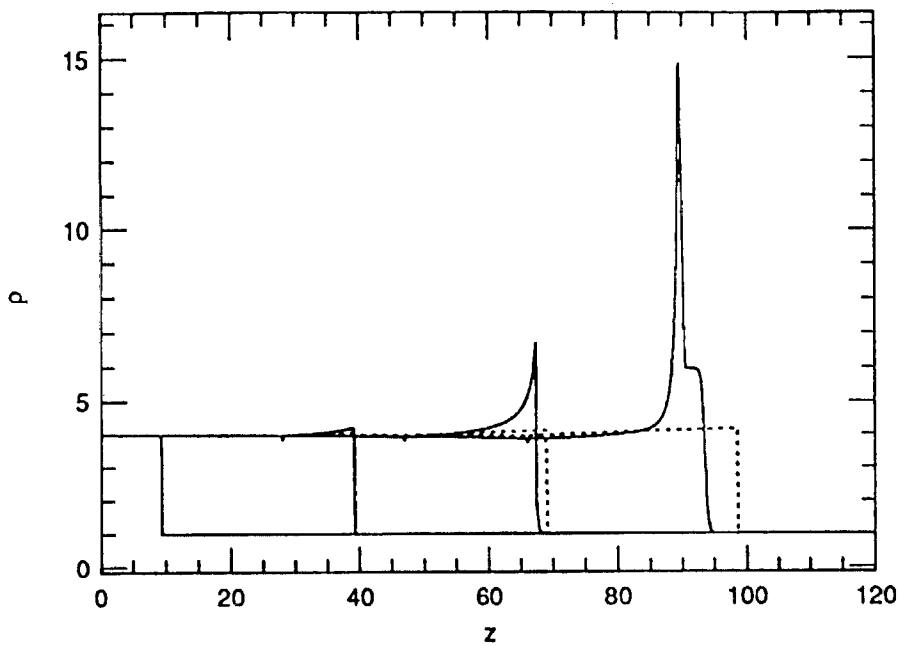
p
z
0
5
10
15
0
20
40
60
80
100
120

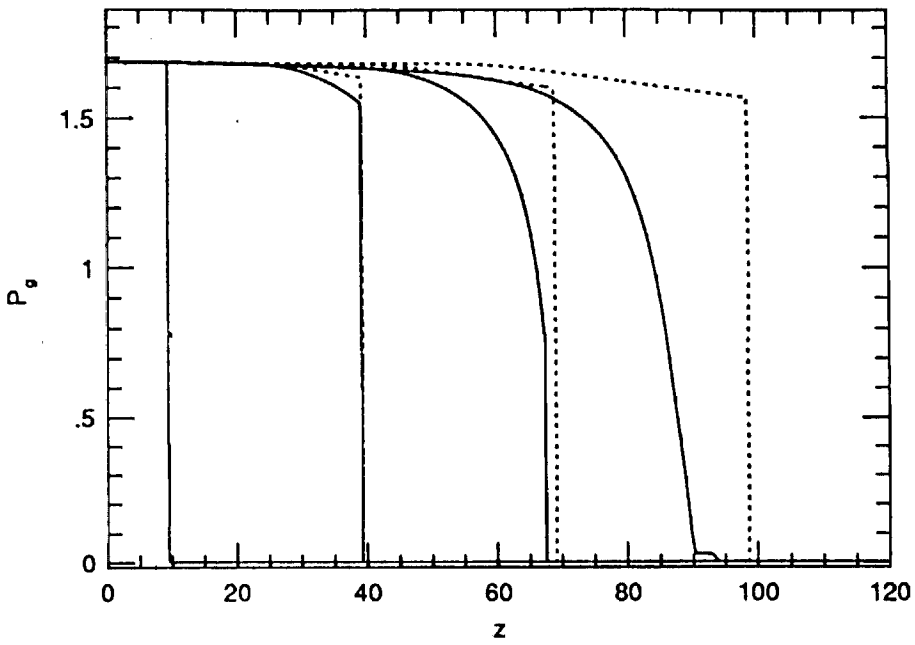
P_g
z
0
.5
1
1.5
0
20
40
60
80
100
120

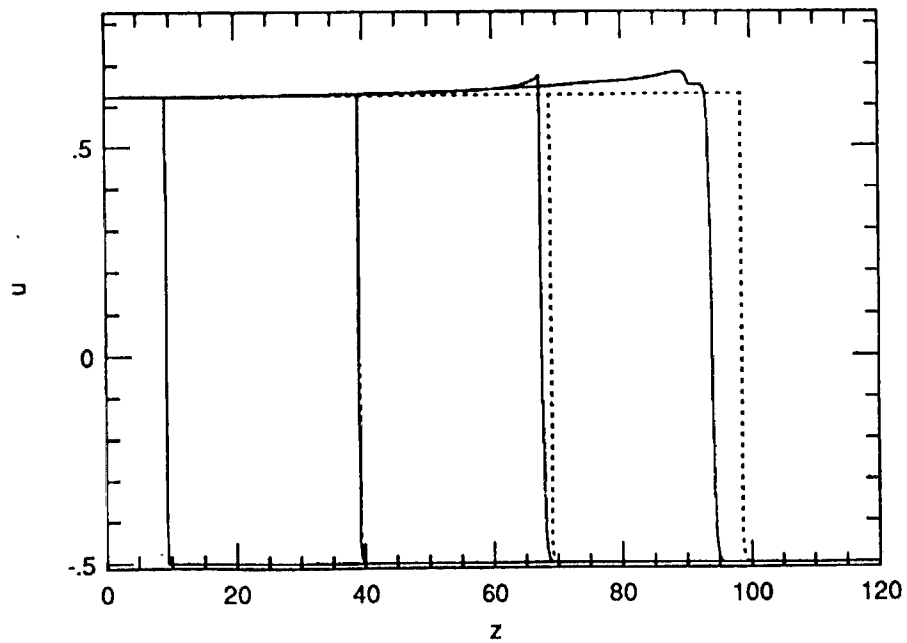
u
z
-.5
0
.5
0
20
40
60
80
100
120

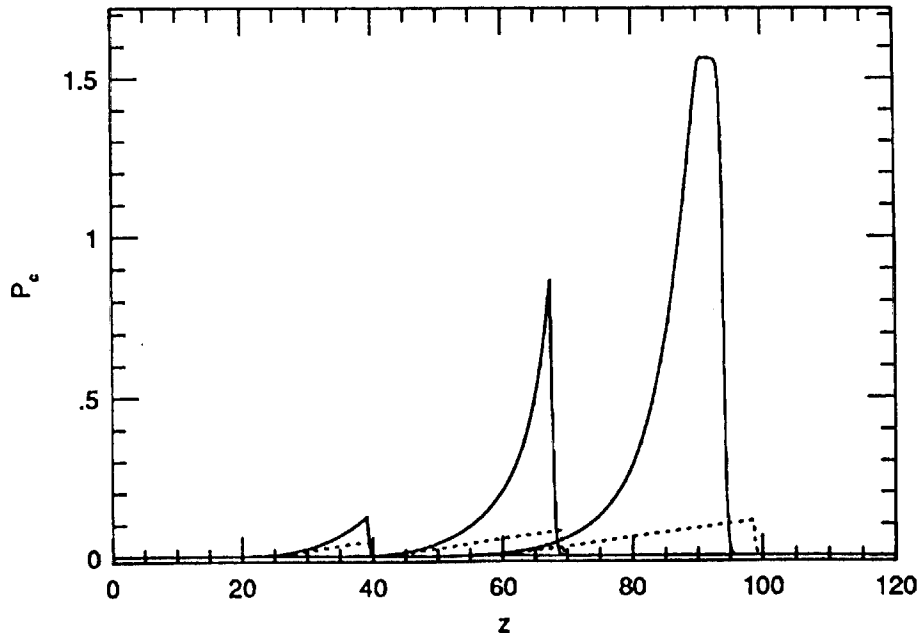
P_e
z
0
.5
1
1.5
0
20
40
60
80
100
120

Figure

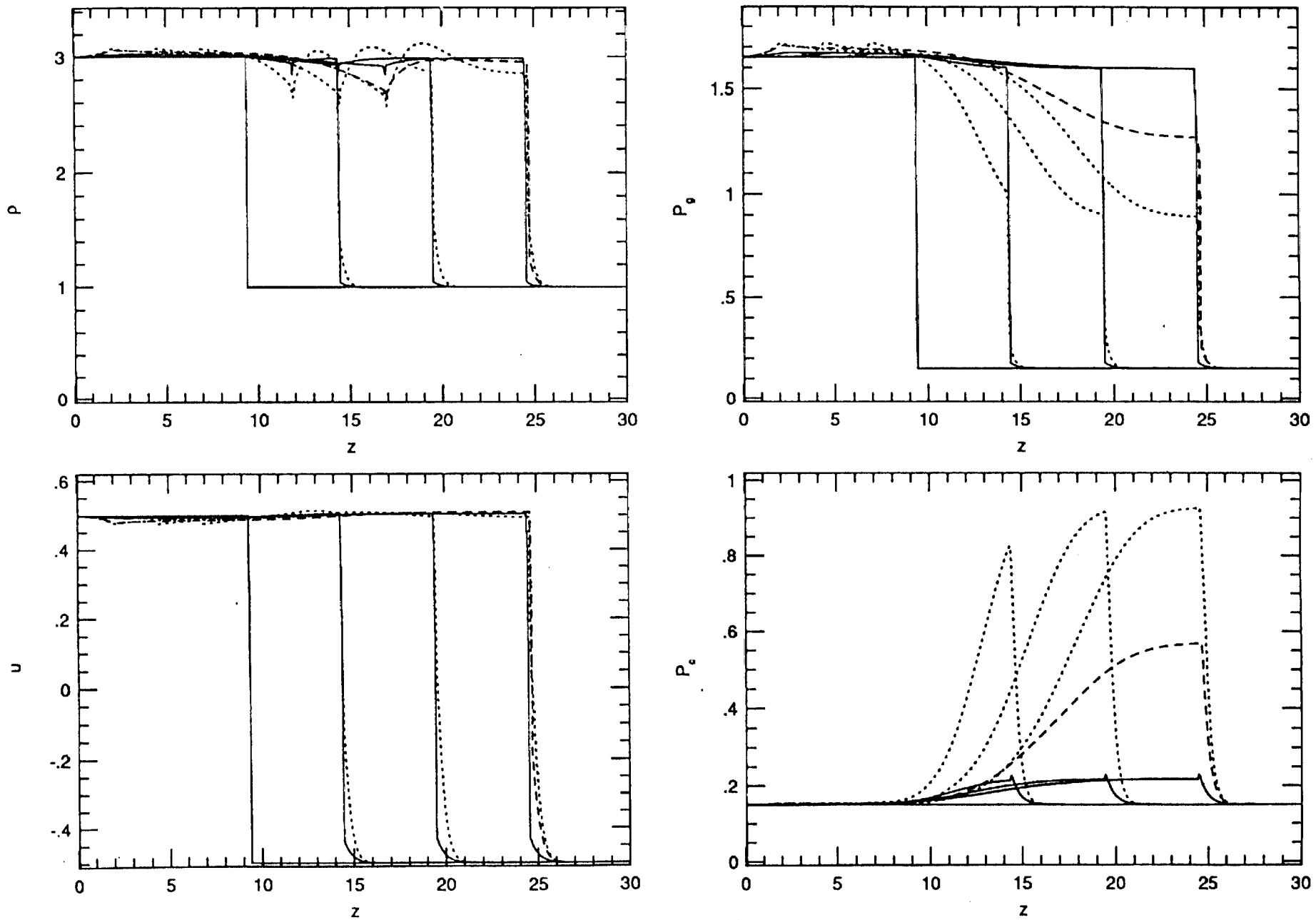

Fig 5

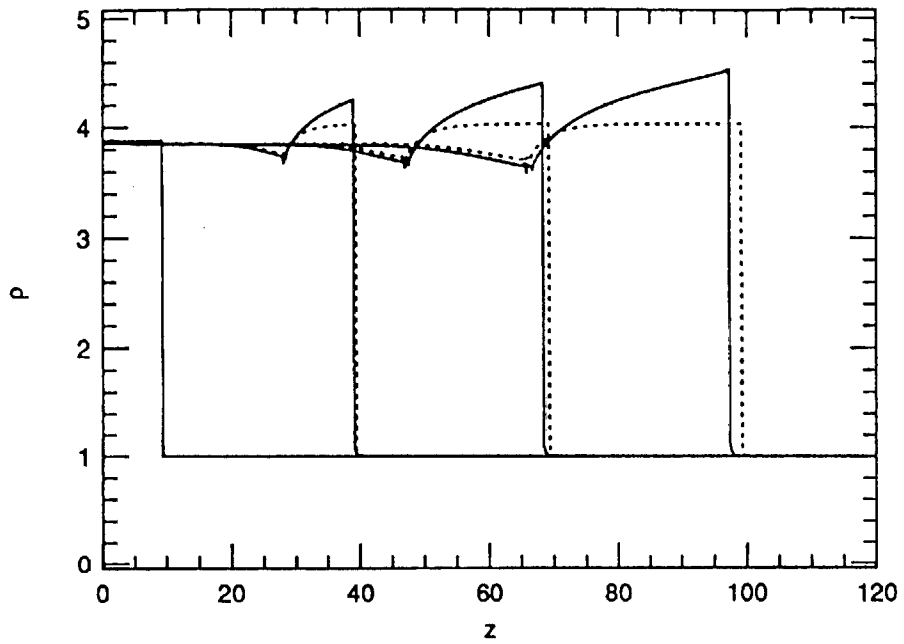
p
z
0
1
2
3
4
5
0
20
40
60
80
100
120

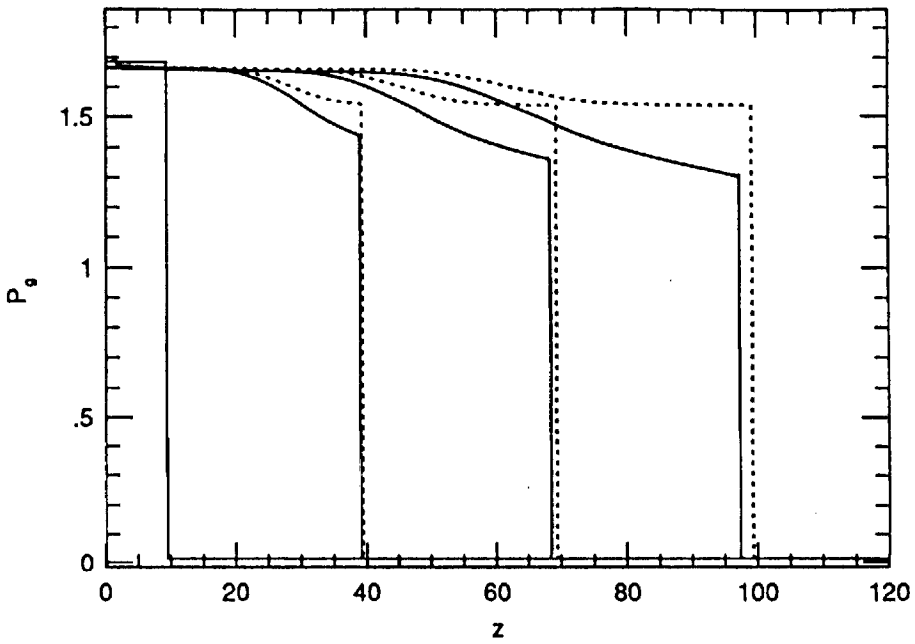
P_a
z
0
.5
1
1.5
0
20
40
60
80
100
120

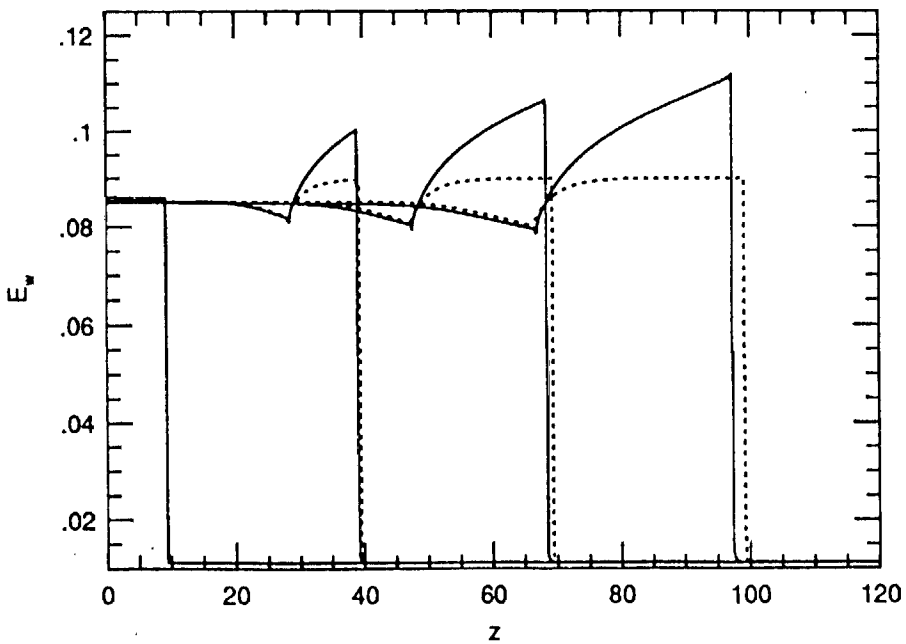
E_w
z
.02
.04
.06
.08
.1
.12
0
20
40
60
80
100
120

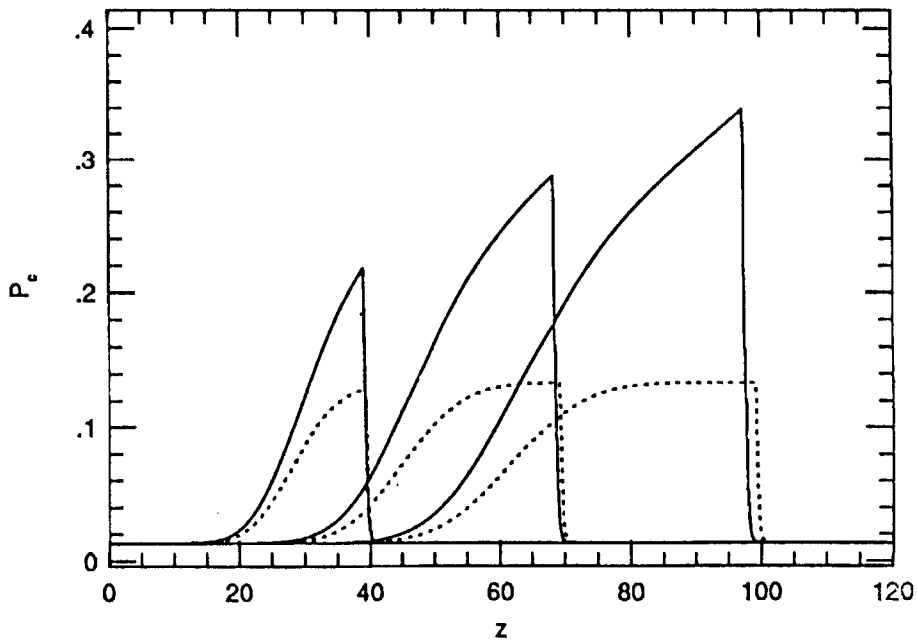
P_e
z
0
.1
.2
.3
.4
0
20
40
60
80
100
120

Fig 6